

Topographic bone thickness maps for Bonebridge implantations

Wilhelm Wimmer · Nicolas Gerber ·
Jérémie Guignard · Patrick Dubach · Martin Kompis ·
Stefan Weber · Marco Caversaccio

Received: 28 November 2013 / Accepted: 20 February 2014
© Springer-Verlag Berlin Heidelberg 2014

Abstract Bonebridge™ (BB) implantation relies on optimal anchoring of the bone-conduction implant in the temporal bone. Preoperative position planning has to account for the available bone thickness minimizing unwanted interference with underlying anatomical structures. This study describes the first clinical experience with a planning method based on topographic bone thickness maps (TBTM) for presigmoid BB implantations. The temporal bone was segmented enabling three-dimensional surface generation. Distances between the external and internal surface were color encoded and mapped to a TBTM. Suitable implant positions were planned with reference to the TBTM. Surgery was performed according to the standard procedure ($n = 7$). Computation of the TBTM and consecutive implant position planning took 70 min on average for a trained technician. Surgical time for implantations under passive TBTM image guidance was 60 min, on average. The sigmoid sinus ($n = 5$) and dura mater ($n = 1$) were exposed, as predicted with the TBTM. Feasibility of the TBTM method was shown for standard presigmoid BB implantations. The projection of three-dimensional bone thickness information into a single topographic map provides the surgeon with an intuitive display of the anatomical situation prior to implantation. Nevertheless, TBTM

generation time has to be significantly reduced to simplify integration in clinical routine.

Keywords Bone-conduction implants · Preoperative planning · Temporal bone · Passive image guidance

Introduction

Bone-conduction implants (BCIs) have become a successful treatment modality for patients suffering from conductive/mixed hearing loss or sensorineural single-sided deafness [1–3]. BCIs improve hearing by transmitting sound through the skull, soft tissues and fluids in the body, ultimately resulting in a vibration of the cochlear basilar membrane [4]. Percutaneous BCIs such as the BAHA® first introduced in 1977 [5] are coupled to the skull by an osseointegrated titanium screw and a skin-penetrating abutment, enabling a direct bone stimulation without damping through soft tissue. However, major disadvantages of percutaneous BCIs include skin infection, skin overgrowth or loss of osseointegration [6, 7]. The next generation of semi-implantable transcutaneous BCIs have therefore been developed to keep the skin intact and overcome the aforementioned drawbacks. Non-active transcutaneous BCIs utilize a passive implant which is driven by an external mechanical transducer [8]. The transducer is magnetically coupled to the implant, requiring a certain transcutaneous static pressure to enable sufficient vibratory signal transmission. Conversely, active transcutaneous BCIs consist of a mechanical transducer which is directly implanted under the skin and fixed to the skull bone, avoiding the mechanical pinching of the skin due to strong pressure between the external and the implanted part [9].

W. Wimmer · N. Gerber (✉) · J. Guignard · S. Weber
ARTORG Center for Biomedical Engineering Research,
University of Bern, Murtenstrasse 50, 3010 Bern, Switzerland
e-mail: nicolas.gerber@artorg.unibe.ch

P. Dubach · M. Kompis · M. Caversaccio
Department of Otorhinolaryngology Head and Neck Surgery,
Inselspital, University of Bern, Bern, Switzerland

P. Dubach
BMBF, Innovation Center for Computer Aided Surgery (ICCAS),
University of Leipzig, Leipzig, Germany

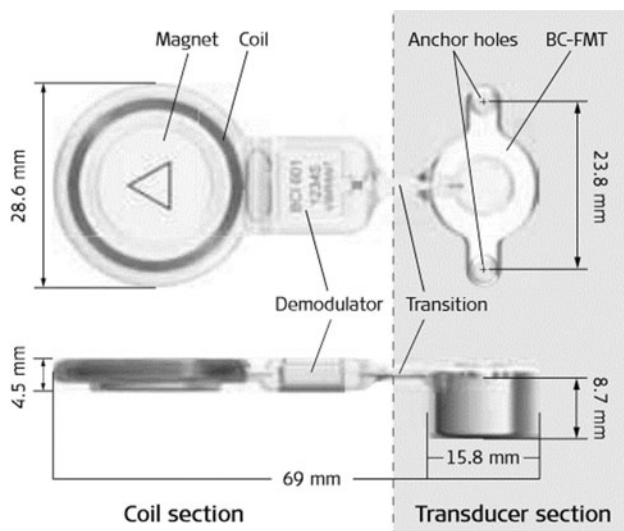


Fig. 1 Implantable component of the Bonebridge™ and floating mass transducer (FMT) dimensions, courtesy of the Vibrant MED-EL Corporation

Recently, an active transcutaneous BCI (Bonebridge™, Med-El Corporation, Innsbruck, Austria) has been reported to achieve hearing restoration comparable to percutaneous BCIs [10–12]. The system consists of an externally worn audio processor and an implantable component incorporating a receiver coil, electronics and an active floating mass transducer (FMT). The FMT is encapsulated within a cylindrical titanium casing (8.7 mm in height and 15.8 mm in diameter) and is anchored in the bone using two self-tapping screws (typically 6 mm length, Fig. 1).

Two different surgical approaches have been proposed for Bonebridge™ (BB) implantation. In the conventional presigmoid approach, the FMT is placed within the mastoid portion of the temporal bone in the so-called sinodural angle, which is limited by the posterior wall of the external auditory canal, the level of the middle fossa dura mater and the sigmoid sinus. The alternative retrosigmoid approach has been tested for patients in which complex radical or obliterated petrosectomy cavities did not allow for fixation in the remaining mastoid bone. Hence, drilling of the implant bed dorsal to the sigmoid sinus was necessary [11, 13]. In both surgical approaches, effective BB implantation requires sufficient space for the FMT as well as tight fixing of the anchoring screws to be implanted. Compared to single-screw percutaneous BCIs, no osseointegration is needed for an effective function, nevertheless, a more advanced surgical procedure under general anesthesia is demanded. Furthermore, preoperative planning is recommended to minimize interference of the FMT with structures of the sigmoid sinus and the dura mater [10, 12].

Current clinical state of the art planning of BB implantations is performed by manual measurements of the bone

thickness in separate two-dimensional axial, coronal or sagittal computed tomography (CT) slices [10]. Optimal position finding of the FMT and the screws under consideration of two-dimensional information requires a complex and cumbersome task to be performed by the surgeon. More suitable planning methods aim to reduce the cognitive task of three-dimensional spatial orientation allowing the surgeon to identify potentially critical contacts of the implant with neighboring anatomical structures. Three-dimensional planning of the implant position using CT image viewers has been reported to overcome these drawbacks. During surgery, transfer of the planned FMT position in situ was either performed with reference to anatomical landmarks [11, 14] or, more invasively, by means of an optical tracking system with a bone-fixed patient reference [13].

Under consideration of minimal invasiveness, a method for a color-encoded representation of the bone thickness in the temporal bone has previously been elaborated for a bone-anchored vascular access port [15]. The technique integrates three-dimensional depth information into a simple topographic bone thickness map (TBTM). A similar utilization of topographic map visualization has been presented within the context of bone density variations in the temporal bone [16]. The TBTM method was evaluated on human cadaver ears with results suggesting that it is a suitable method for skull base implant position planning. The method provides the surgeon with information for the preoperative planning process and intraoperative situs orientation, while avoiding additional invasive procedures to the patient.

This study aims to evaluate the clinical applicability of BB implantation planning based on TBTM findings. It is hypothesized that the method is able to give an intuitive overview of the anatomical situation prior to surgery and aid the surgeon to identify suitable implantation areas. Further, the FMT coupling efficacy is evaluated using postoperative audiometric testing.

Materials and methods

Study subjects

Between November 2012 and September 2013, seven patients selected for presigmoid BB implantation were included in the study (data summarized in Table 1). All patients underwent preoperative audiometric evaluation and successfully passed a trial phase with head-band bone-conduction hearing aids. Patients with mixed/conductive hearing loss ($n = 3$) fulfilled the audiometric selection criteria for BB implantation, presenting bone-conduction thresholds of the ipsilateral ear within 45 dB HL between 500 and 4,000 Hz. Three patients with single-sided

Table 1 Study subject details

| Subject no. | Age at surgery (years) | Gender | Implanted ear side | Type of hearing loss | Etiology | Preoperative image data |
|-------------|------------------------|--------|--------------------|----------------------|----------------------|-------------------------|
| 01 | 19 | F | R | CHL | Microtia/atresia | CT |
| 02 | 41 | F | R | SSD | Labyrinthitis | CBCT |
| 03 | 56 | M | L | SSD | Parotid tumor | CT |
| 04 | 72 | F | L | SSD | Mumps | CBCT |
| 05 | 18 | M | R | MHL | Microtia/atresia | CBCT |
| 06 | 19 | M | R | CHL | Chronic otitis media | CBCT |
| 07 | 54 | F | R | SSD | Sudden hearing loss | CBCT |

CHL conductive hearing loss, MHL mixed hearing loss, SSD sensorineural single-sided deafness, CT computed tomography, CBCT cone-beam CT

deafness had air-conduction thresholds equal to or better than 20 dB HL between 500 and 4,000 Hz in the contralateral ear. One patient presented single-sided deafness in combination with high-frequency hearing loss in the better ear (subject 04, hearing threshold of 30 dB HL at 2,000/3,000 Hz and 50 dB HL at 4,000 Hz). All implanted candidates objected to the alternative of a conventional percutaneous BCI because of the stigmatization by the visible screw. Secondary reason to opt for BB implantation was to avoid the need for life-long screw care with the possible risk of local infection or screw extrusion. The study protocol was conducted according to the standards of the Declaration of Helsinki 1964.

Preoperative imaging

Preoperative CT scans ($0.40 \times 0.40 \times 0.40 \text{ mm}^3$, $V = 120 \text{ kVp}$, $I = 120 \text{ mA}$) or cone-beam CT scans ($0.15 \times 0.15 \times 0.15 \text{ mm}^3$, $V = 96 \text{ kVp}$, $I = 12 \text{ mA}$) have been used if they were not older than 3 months. If pre-existing CTs were not available, cone-beam CT imaging of the lower skull was performed on the day before surgery following the routine protocol.

Preoperative planning procedure

Preoperative planning was performed at least 1 day before surgery. The following planning steps were adapted from [15] and performed with Amira® visualization software (VSG, Burlington, MA, USA). To provide a quick structural overview of the implantation site, the skull bone was segmented with thresholding, followed by three-dimensional surface generation. Using the computed surface, image data were cropped to a retroauricular volume of interest, limited anteriorly by the external auditory canal, caudally by the mastoid tip, cranially by the level of the zygomatic process and posteriorly by the occipitomastoid suture. Due to the heterogeneity of pneumatization of the temporal bone (i.e., mastoid air cells and middle

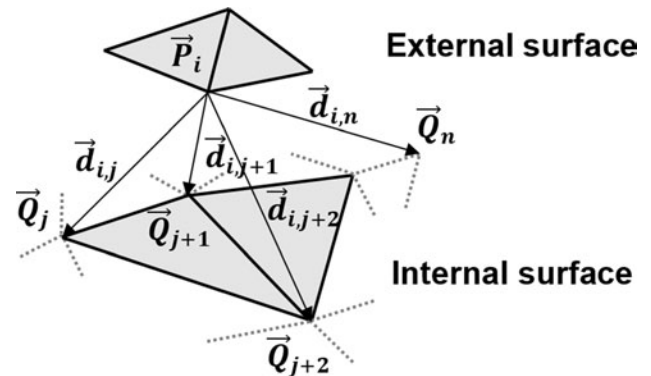


Fig. 2 Graphical representation of the minimum Euclidean distance computation

ear cavity), manual correction of the labels found by the thresholding algorithm was necessary. In CT slices where the thresholding algorithm did not generate continuous edges between bone and soft tissue, the labels were edited by free-hand drawing on the slice to correct border, mastoid cortex and air cells artifacts. A three-dimensional surface was generated for the volume of interest, depicting potentially available space for implantation. The outer surface of the skull and the surface of intracranial soft tissue structures (sigmoid sinus and dura) were manually separated and the bone thickness was calculated as the smallest Euclidean distance between the vertices of both meshes (Fig. 2). The minimal distance (d_i) between a vertex on the outer surface (\vec{P}_i) and n vertices on the internal surface (\vec{Q}_j) can be obtained according to Eq. (1).

$$d_i = \min_{j=1, \dots, n} \|\vec{d}_{i,j}\|_2 = \min_{j=1, \dots, n} \|\vec{P}_i - \vec{Q}_j\|_2 \tag{1}$$

The obtained distances were mapped to the outer surface, color encoded according to the bone thickness and displayed as TBTM. Suitable regions for FMT and screw implantation were indicated following the colors defined in Table 2.

Table 2 Bone thickness, corresponding colors and surgical implications of the topographic bone thickness map (TBTM)

| Bone thickness (mm) | Color | Surgical implication |
|---------------------|--------|---|
| ≤ 4 | Red | Unsuitable for screw or FMT placement |
| 4–6 | Yellow | Sufficient bone thickness for screw placement, unsuitable for FMT placement |
| 6–8 | White | Expected interference with sigmoid sinus or dura mater |
| ≥ 9 | Green | Sufficient bone thickness for FMT placement |

FMT floating mass transducer

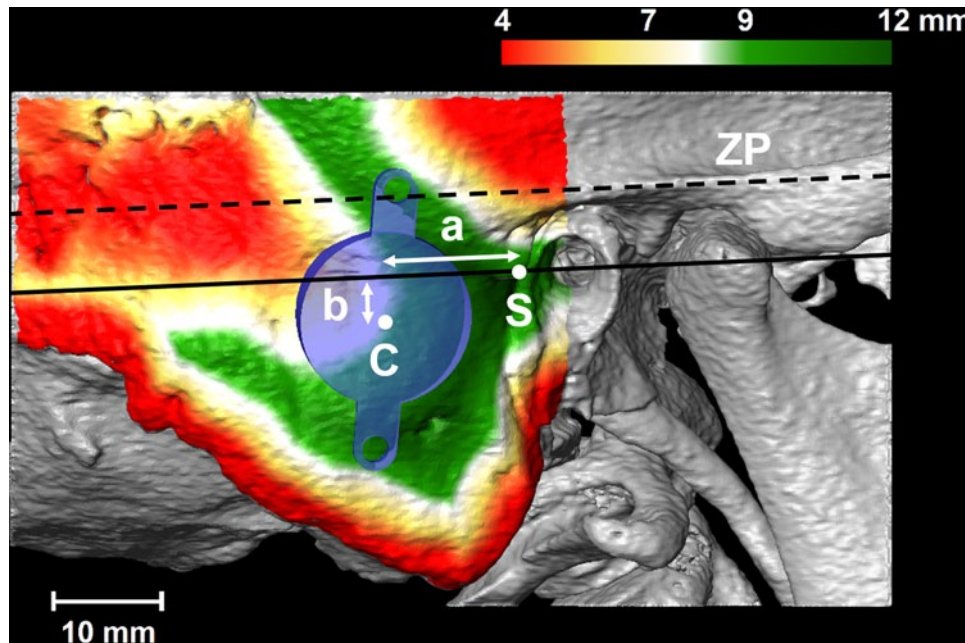


Fig. 3 Preoperative plan of a temporal bone with topographic bone thickness map (TBTM, subject 06, right side). The bone thickness in the mastoid region is color encoded ranging from 4 to 12 mm. Green areas depict sufficient bone thickness (≥ 9 mm) for placement of the floating mass transducer (FMT, blue representation). White (6–8 mm), yellow (4–6 mm) and red (≤ 4 mm) areas provide the sur-

geon with information about expected interference with the sigmoid sinus or dura mater. A reference coordinate system is orientated with respect to the temporal line and zygomatic process (ZP). The Cartesian distances (a , b) between the FMT center point (C) and Henle's spine (S) are measured for intraoperative implant position finding

Using the TBTM, a three-dimensional model of the FMT was imported and positioned at a suitable implantation location. The FMT was preferably positioned between the temporal line and the insertion of the sternocleidomastoid muscle to reduce implantation depth. Minimization of contact with the sigmoid/transverse sinus and the dura mater was achieved through placement within green areas of the TBTM (Fig. 3). Besides sufficient embedding and smooth surface alignment of the FMT, adequate bone thickness at the screw positions (at least yellow areas) was decisive for position planning. A reference coordinate system determined by easily identifiable anatomical landmarks was used to enable intraoperative transfer of the planned implant position. The coordinate system was oriented with respect of to the temporal line/zygomatic process and the Cartesian distances between the FMT center and Henle's spine were measured (Fig. 3). The planned implant position

in the TBTM was reviewed and optimized by the surgeon. The total preoperative planning time including image segmentation and implant positioning was recorded for later evaluation.

Surgical procedure

During surgery, the final surgical plan was displayed to the surgeon on a display monitor. BB surgery followed a standardized protocol. Using a retroauricular approach, an L-shaped skin incision and musculo-periosteal flap were created. After careful hemostasis and denudation of the planum mastoideum, the anatomical landmarks defined in the preoperative plan were identified (i.e., Henle's spine, level of zygomatic process and temporal line). The center point of the FMT was transferred with reference to the planning coordinates using a surgical ruler and pen. A FMT dummy

Table 3 Summary of preoperative predictions and intraoperative findings for all implantation cases

| Subject no. | TBTM planning (min) | Operative time (min) | FMT center position | | Sigmoid sinus exposed | Dura mater exposed |
|-------------|---------------------|----------------------|---------------------|---------------|-----------------------|--------------------|
| | | | <i>a</i> (mm) | <i>b</i> (mm) | | |
| 01 | 90 | 80 | 14 | 8 | TP | TN |
| 02 | 85 | 100 | 11 | 3 | TP | TP |
| 03 | 70 | 50 | 20 | 5 | TP | TN |
| 04 | 70 | 45 | 16 | 9 | TN | TN |
| 05 | 60 | 45 | 16 | 8 | TP | TN |
| 06 | 65 | 50 | 12 | 4 | TP | TN |
| 07 | 60 | 40 | 15 | 3 | TN | TN |
| Avg. ± SD | 71 ± 12 | 59 ± 22 | 14.9 ± 3.0 | 5.7 ± 2.6 | <i>n</i> = 5 (TP) | <i>n</i> = 1 (TP) |

TBTM topographic bone thickness map, TP true positive (structure was exposed, as expected), TN true negative (structure was unexposed, as expected)

provided with the implantation kit was used to indicate the milling area and screw positions on the bone surface. The implant bed was carefully milled out for close fitting and preservation of maximal bone rim for screw fixation. Bone dust was collected at this stage for potential bone augmentation of the drilled cavity. The base of the bed was gently milled using a diamond drill to avoid accidental contact with the sigmoid sinus or dura mater. After completion of the implant bed, the FMT was positioned and the flexible transition to the receiving coil/demodulator was bent to fit below the musculo-periosteal flap. The FMT was fixed using two self-tapping bone screws (penetration depth 4 mm). Finally, the flap was closed with subcutaneous and cutaneous sutures. All implantations were performed under general anesthesia. The size and position of the milled implant bed was photo-documented and compared with the plan intraoperatively. The surgical time, expected/unexpected interference with anatomical structures and deviations from the standard surgical procedure were recorded. No radiologic postoperative control was performed to avoid additional radiation exposure to the patients.

Audiological evaluation

All implants were activated and fitted 1 month after surgery. Individual optimization of the audio processor fitting took place in further two sessions after 1 month each. Audiological evaluation was performed in a sound-attenuated room using calibrated equipment according to ISO 8253 series. To assess coupling efficacy and performance of the implant, aided and unaided sound field hearing thresholds were measured at 250, 500, 1,000, 2,000, 3,000, 4,000, and 6,000 Hz using narrow-band noise. Noise-reduction algorithms of the external audio processor were deactivated during measurements. The mean observation period for audiometric evaluation of the BB performance and patient satisfaction assessment took place 7 weeks after activation.

Results

Preoperative planning time for TBTM generation and optimal FMT positioning took about 70 min on average (Table 3), mainly caused by the required manual correction of segmentation labels after thresholding. The TBTM method was successfully implemented in the surgical process and provided the surgeon an immediate understanding of the anatomical situation at the implantation site. A suitable implant position was found in every case. Critical zones for implant bed milling and expected interference with the sigmoid sinus or dura mater were identified prior to implantation using the TBTM in a short preoperative review time (5–10 min).

Transfer of the planned FMT position was achieved in all cases using the anatomical landmark reference. The average FMT center position was found to be at distances $a = 14.9$ and $b = 5.7$ mm (Table 3) from the Henle's spine. Intraoperative observations generally matched the implications given by the TBTM. Two surgeries were considered challenging regarding safe placement of the FMT because of limited space in the mastoid region (subjects 01 and 02). Skeletonization of the dura mater was necessary in a single case only (subject 02, Fig. 4). However, interference with the sigmoid sinus was expected and encountered in the majority of cases ($n = 5$). In one case, only partial embedding of the FMT was achievable due to a small skull size, as anticipated with the TBTM (subject 02, Fig. 5). This led to an implant protrusion of about 2 mm over the skull surface. Full embedding of the implant was achieved using a substitute material for bone regeneration (Bio-Oss[®], Geistlich Pharma, Wolhusen, Switzerland) and a caudal anchoring screw with 10 mm length (6 mm penetration depth). In two cases, the caudal screws ended up in a mastoid air cell impeding firm tightening and had to be replaced with 2 mm longer screws (i.e., 8 mm length, subjects 04 and 07). All surgeries were performed without compression of the dura mater or the sigmoid sinus.

Fig. 4 Topographic bone thickness map (TBTM) in case with limited space, planned implant position (*blue*) and corresponding intraoperative photo-documentation (subject 01). The zygomatic process (*ZP*) and temporal line served as FMT position reference. As indicated by the TBTM, the sigmoid sinus (*ss*) and the dura mater (*dm*) were exposed during implant bed milling (*upper photo*). Full embedding and fixation of the FMT was achieved during surgery (*lower photo*)

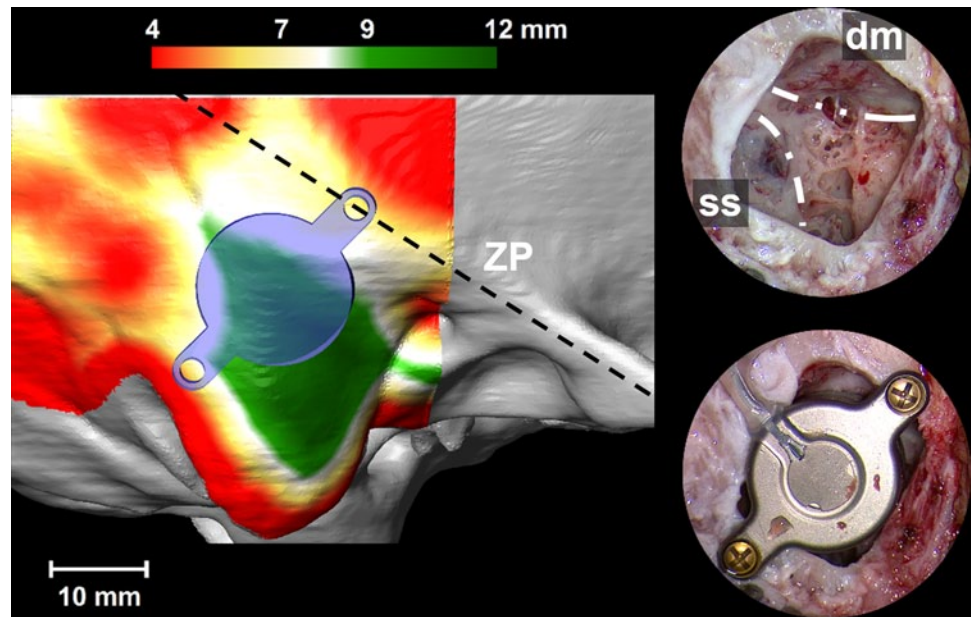
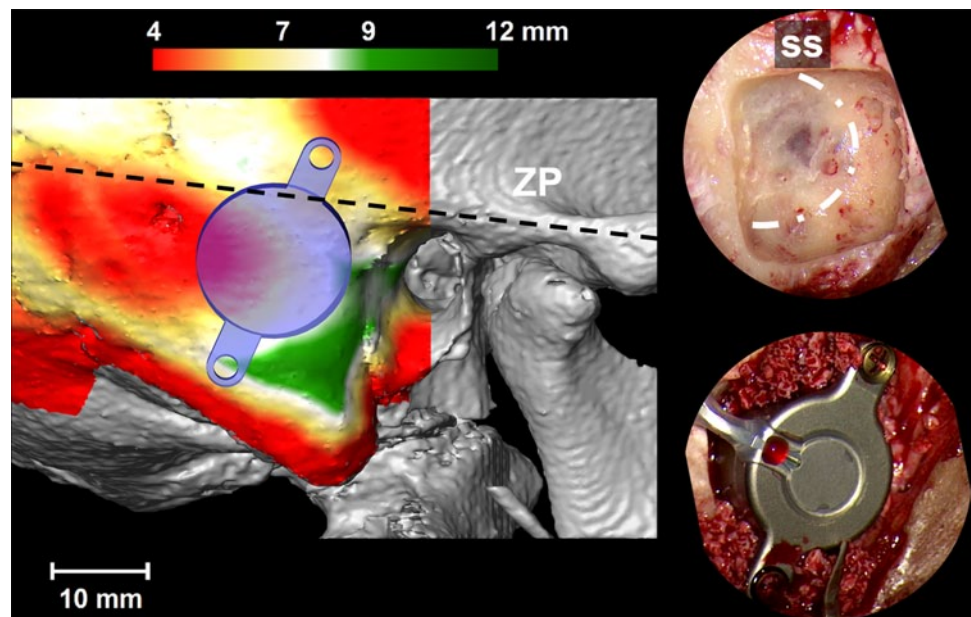


Fig. 5 Case of implant with protrusion of 2 mm over bone surface (subject 02). As indicated by the topographic bone thickness map (TBTM), full embedding of the implant without compression of the sigmoid sinus was not possible. Transfer of the implant position (*blue*) was performed with reference to the zygomatic process (*ZP*) and temporal line. The sigmoid sinus (*ss*) was exposed as expected (*upper photo*) and the implant was fully embedded using an artificial bone regeneration material (*lower photo*)



No intraoperative complications or postoperative infections occurred. None of the patients complained about postoperative skin irritation, wound infection or headache. Sound field hearing performance showed an average improvement of 29.7 dB between 500 and 4,000 Hz. All patients reported on complete toleration of their everyday sound environment.

Discussion

This work presents the next step in the clinical investigation of the TBTM method following a pre-clinical feasibility

study performed on whole-head cadaver specimens. The influence of partial volume effect artifacts and segmentation errors has been previously reported to be negligible [15].

The main advantage of the TBTM method is the intuitive presentation of the bone thickness at the implantation site. Using the TBTM, suitable implant positions can be distinguished from critical implantation areas in a short preoperative reviewing time. During surgery, the spatial awareness of the surgeon can be improved without further procedures (e.g., attachment of patient markers or special tracking equipment) or additional radiation exposure. Especially for BB implantations in pediatric cases, where

confronted with smaller dimensions of the temporal bone, the planning method could add important information to the surgeon preoperatively. The TBTM method could indicate whether surgery in a given patient is not recommended for anatomical reasons, which offers a clear advantage compared to aborting an ongoing surgery. This situation, however, did not happen in our experience.

Manual transfer of the planned implant position as described in this work was sufficient for BB surgery. The presented planning coordinate system uses Henle's spine as reference, but can be adapted to other available anatomical landmarks (e.g., skull sutures or posterior wall of the external auditory canal). This may be the case if BB implantation is performed in a temporal bone with a previous mastoidectomy or parotidectomy.

Compared to the average surgical duration of BB implantations (60 min) the generation of the TBTM is a relatively long procedure (70 min). The most time-consuming part of the method is the manual revision of the bone segmentation labels. The temporal bone is a heterogeneous and highly pneumatized structure (mastoid air cells, middle ear cavity) and requires profound anatomical knowledge for segmentation. For this reason, it is difficult to apply automatic segmentation algorithms [17]. Both of the drawbacks, the time consumption and the required training level may affect the integration into clinical routine. Nevertheless, the implementation of (semi-)automatic methods may significantly reduce the impact of the mentioned disadvantages [17–19] and is thus currently under investigation.

As reported in previous work, BB implantation is considered a safe surgical procedure in both the presigmoid [10, 11] and the retrosigmoid approach [13, 14]. Challenging cases were identified preoperatively using the TBTM and the surgical procedure was adapted accordingly. A strict presigmoid implantation paradigm with focus on avoidance of soft tissue compressions was followed during surgeries. Long-term results of BAHA® implantations suggest that contact to the sigmoid sinus or the dura mater rarely results in complications [6]. However, compression of the sigmoid sinus could theoretically lead to thrombosis. Patient 06 presented chronic otitis media in a stable condition (no secretion over 3 years), localized in the tympanic cavity only, without secretion in the mastoid air cells (based on CT imaging). During surgery, special care was taken to avoid an opening of the antrum block during implant bed milling. Nevertheless, a potential risk of biofilm formation, infection or discharge of the implant exists. Considering a possible compression of the dura, a retrosigmoid BB implantation would be an alternative option. In case of a favored retrosigmoid approach, the TBTM may also provide useful information for implant position planning.

The Med-El Corporation provides a tutorial together with a FMT model for preoperative planning of BB

implantations using the open-source software 3D Slicer (<http://www.slicer.org>). Compared to the presented TBTM method, it is freely available. Nevertheless, the method does not provide an intuitive visual feedback about the available bone thickness. The presented TBTM method is not limited to the Amira® software and could be as well implemented in open-source software solutions (e.g., 3D Slicer).

Conclusions

In this work, the feasibility and clinical reliability of the TBTM method for preoperative planning of BB implantations have been shown. Effective coupling of the FMT in the temporal bone was shown through the improvement of sound field hearing thresholds. Especially in challenging situations (i.e., small skulls) the method is a viable tool to support surgeons and may contribute to a higher patient safety. Regarding the long time taken to generate the TBTM, a significant reduction of the procedural duration is demanded to increase acceptance of clinicians.

Conflict of interest The authors declare that they have no conflict of interest.

References

- Piffner F, Caversaccio MD, Kompis M (2011) Audiological results with Baha® in conductive and mixed hearing loss. In: Kompis M, Caversaccio M (eds) Implantable bone conduction hearing aids. *Adv Otorhinolaryngol*, vol 71. Karger, Basel, pp 73–83
- Wazen JJ, Spitzer JB, Ghossaini SN, Fayad JN, Niparko JK, Cox K, Brackmann DE, Soli SD (2003) Transcranial contralateral cochlear stimulation in unilateral deafness. *Otolaryngol Head Neck* 129:248–254
- Yuen HW, Bodmer D, Smilsky K, Nedzelski JM, Chen JM (2009) Management of single-sided deafness with the bone-anchored hearing aid. *Otolaryngol Head Neck* 141:16–23
- Stenfelt S (2011) Acoustic and physiologic aspects of bone conduction hearing. In: Kompis M, Caversaccio M (eds) Implantable bone conduction hearing aids. *Adv Otorhinolaryngol*, vol 71. Karger, Basel, pp 10–21
- Tjellström A, Lindström J, Hallén O, Albrektsson T, Brånemark PI (1981) Osseointegrated titanium implants in the temporal bone. A clinical study on bone-anchored hearing aids. *Am J Otolaryngol* 2:308–310
- Wazen JJ, Wycherly B, Daugherty J (2011) Complications of bone-anchored hearing devices. In: Kompis M, Caversaccio M (eds) Implantable bone conduction hearing aids. *Adv Otorhinolaryngol*, vol 71. Karger, Basel, pp 63–72
- Kraai T, Brown C, Neeff M, Fisher K (2011) Complications of bone-anchored hearing aids in pediatric patients. *Int J Pediatr Otorhinolaryngol* 75:749–753
- Denoyelle F, Leboulanger N, Coudert C, Mazzaschi O, Loundon N, Vicaut E, Tessier N, Garabedian EN (2013) New closed skin bone-anchored implant: preliminary results in 6 children with ear atresia. *Otol Neurotol* 34:275–281

9. Håkansson B, Reinfeldt S, Eeg-Olofsson M, Östli P, Taghavi H, Adler J, Gabrielsson J, Stenfelt S, Granström G (2010) A novel bone conduction implant (BCI): engineering aspects and pre-clinical studies. *Int J Audiol* 49:203–215
10. Sprinzl G, Lenarz T, Ernst A, Hagen R, Wolf-Magele A, Mojallal H, Todt I, Mlynski R, Wolfram M (2013) First European multicenter results with a new transcutaneous bone conduction hearing implant system: short-term safety and efficacy. *Otol Neurotol* 34:1076–1083
11. Barbara M, Perotti M, Gioia B, Volpini L, Monini S (2013) Transcutaneous bone-conduction hearing device: audiological and surgical aspects in a first series of patients with mixed hearing loss. *Acta Otolaryngol* 133:1058–1064
12. Huber AM, Sim JH, Xie YZ, Chatzimichalis M, Ullrich O, Rösli C (2013) The Bonebridge: preclinical evaluation of a new transcutaneously-activated bone anchored hearing device. *Hear Res* 301:93–99
13. Canis M, Ihler F, Blum J, Matthias C (2013) CT-assisted navigation for retrosigmoidal implantation of the Bonebridge. *HNO* 61:1038–1044
14. Lassaletta L, Sanchez-Cuadrado I, Muñoz E, Gavilan J (2014) Retrosigmoid implantation of an active bone conduction stimulator in a patient with chronic otitis media. *Auris Nasus Larynx* 41:84–87
15. Guignard J, Arnold A, Weisstanner C, Caversaccio M, Stieger C (2013) A bone thickness map as a guide for implantation surgery in the temporal bone. *Materials* 6:5291–5301
16. Sprinzl G, Mockenhaupt J, Koebeke J, Thumfart WF (1992) The temporal bone. *HNO* 40:206–214
17. Salah Z, Kastner M, Dammann F, Schwaderer E, Maassen MM, Bartz D, Strasser W (2006) Preoperative planning of a complete mastoidectomy: semiautomatic segmentation and evaluation. *Int J Cars* 1:213–222
18. Gerber N, Bell B, Gavaghan K, Weisstanner C, Caversaccio M, Weber S (2014) Surgical planning tool for robotically assisted hearing aid implantation. *Int J Cars* 9:11–20
19. Reda FA, Noble JH, Rivas A, McRackan TR, Labadie RF, Dawant BM (2011) Automatic segmentation of the facial nerve and chorda tympani in pediatric CT scans. *Med Phys* 38:5590–5600